



### **Science Arts & Métiers (SAM)**

is an open access repository that collects the work of Arts et Métiers Institute of Technology researchers and makes it freely available over the web where possible.

This is an author-deposited version published in: <https://sam.ensam.eu>  
Handle ID: <http://hdl.handle.net/10985/8257>

#### **To cite this version :**

Philippe VIOT - Hydrostatic compression on polypropylene foam - International Journal of Impact Engineering - Vol. 36, n°7, p.975-989 - 2008

Any correspondence concerning this service should be sent to the repository

Administrator : [scienceouverte@ensam.eu](mailto:scienceouverte@ensam.eu)



---

# Hydrostatic compression on polypropylene foam

Philippe Viot

LAMEFIP, ENSAM de BORDEAUX, Esplanade des Arts et Métiers, 33405 Talence Cedex, France

---

## A B S T R A C T

Models currently used to simulate the impact behaviour of polymeric foam at high strain rates use data from mechanical tests. Uniaxial compression is the most common mechanical test used, but the results from this test alone are insufficient to characterise the foam response to three-dimensional stress states. A new experimental apparatus for the study of the foam behaviour under a state of hydrostatic stress is presented. A flywheel was modified to carry out compression tests at high strain rates, and a hydrostatic chamber designed to obtain the variation of stress with volumetric strain, as a function of density and deformation rate. High speed images of the sample deformation under pressure were analysed by image processing.

Hydrostatic compression tests were carried out, on polypropylene foams, both quasi statically and at high strain rates. The stress–volumetric strain response of the foam was determined for samples of foam of density from 35 to 120 kg/m<sup>3</sup>, loaded at two strain rates.

The foam response under hydrostatic compression shows a non-linear elastic stage, followed by a plastic plateau and densification. These were characterised by a compressibility modulus (the slope of the initial stage), a yield stress and a tangent modulus. The foam was transversely isotropic under hydrostatic compression.

---

### Keywords:

Polymeric foam

Cellular material

Hydrostatic compression

Strain rate

Dynamic loading

---

## 1. Introduction

Polymer foams are used in a number of applications; consumer goods packaging for electronic equipment, or consumer passive protection helmets, knee pads..., due to their good energy absorbing capability during a shock. To improve the quality and the performance of these products, numerical modelling can be used. However, the stress conditions during an impact must be defined and a precise knowledge of the mechanical characteristics of the foam used in these structures is required.

The behaviour of these polymer foams depends on the type of loading, the foam density, the imposed strain rate and the temperature. Many authors have studied the effect of density by carrying out uniaxial compression tests on samples of variable densities [1]. However, there have been few results for compressions at impact strain rates [2,3]. This is the information of most interest to designers of helmets etc, because it will help them to make an optimum choice of material.

The macroscopic behaviour of polymer foams classically shows three regimes (Fig. 1) [1]: an elastic region followed by a stress plateau  $\sigma_{pl}$  (where the stress  $\sigma$  is nearly constant for a large range of strain  $\epsilon$ ) corresponding to plastic yielding, and densification. In passive safety applications, the plastic plateau behaviour allows the dissipation of the mechanical energy for a nearly constant

stress. Consequently, the elastic and plateau regimes have to be characterised.

During impacts on foam products, the stress state is often triaxial, rather than uniaxial compression. Constitutive models for cellular materials have been investigated: Gibson et al. [4], Zhang et al. [5] and Triantafillou et al. [6] studied the behaviour of polymeric and metallic foams under multi-axial loading and for different strain rate conditions, and proposed yield surfaces. Gibson and Ashby studied polyurethane, polyethylene and aluminium foams (closed or open cells) and established constitutive equations based on the analysis of the mechanical response of an ideal foam structure. Zhang et al. carried out a large campaign of uniaxial tension and compression, hydrostatic compression and shear tests on polypropylene, polystyrene and polyurethane foams and proposed a rate dependent constitutive equation. In all cases, the yield surface is an ellipse in the hydrostatic/deviatoric plane. These results were confirmed by Miller [7] who derived an elliptical yield surface to describe cellular materials or foamed cells. Deshpande and Fleck [8] developed isotropic constitutive models for metallic foams and studied the change of the yield surface in stress space, taking into account differential hardening along the hydrostatic and deviatoric axes. For wood, which can be considered as a cellular material, a constitutive model was modified by Tagarielli et al. [9] to represent the behaviour of transversely isotropic foams.

Some of these models have been implemented in Finite Element codes such as ABAQUS [10] and LS DYNA [11]. The mechanical

---

E-mail address: philippe.viot@lamef.bordeaux.ensam.fr

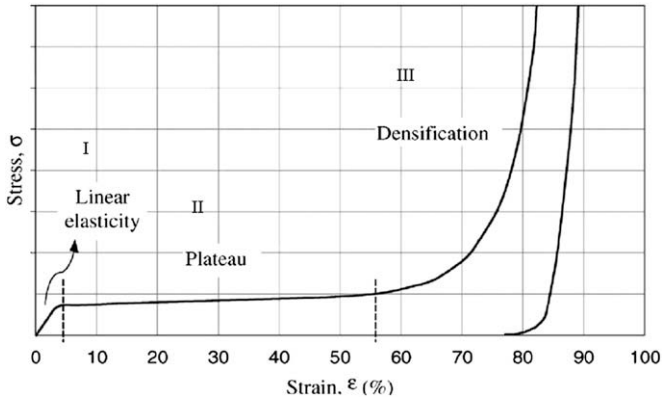


Fig. 1. Classical stress versus strain behavior of cellular material under uniaxial compression.

parameters of these numerical models  $\underline{\sigma} = f(\underline{\varepsilon})$ , linking the stress tensor  $\underline{\sigma}$  and strain tensor  $\underline{\varepsilon}$ , must be identified as functions of variables such as the strain rate, temperature and density of the cellular material. One method of characterisation consists of performing a number of mechanical tests in order to determine the model parameters. A second, inverse method of model characterisation compares the results of modelling a complex loading on a foam structure with the experimental response of this structure. The model parameters are adjusted to obtain the best correlation between numerical and experimental results. This approach was applied by Jin et al. [12] to identify the mechanical behaviour of polyurethane foams.

The first method of parameter characterisation was used in this paper, using different loading paths in a hydrostatic stress–deviatoric stress plane. The yield surface of the constitutive model can be described by an ellipse in the planes  $p$ – $q$  (where the hydrostatic stress  $p = (1/3)\text{tr}(\underline{\sigma})$  and  $q = ((3/2)\underline{\tilde{\sigma}} : \underline{\tilde{\sigma}})^{1/2}$  if  $\underline{\tilde{\sigma}}$  is the deviatoric stress tensor, Fig. 2). The characterisation of this surface requires at least three mechanical tests. The uniaxial compression test is strongly deviatoric (point 1, Fig. 2); the hydrostatic stress is  $p = \sigma_z/3$  whereas  $q = \sigma_z$ , where  $\sigma_z$  is the axial stress.

A hydrostatic compression test provides further experimental data (point 2 Fig. 2). Hydrostatic compression is defined by:

$$p = P \text{ and } q = 0 \text{ where } P \text{ is the pressure applied on the material.}$$

Hydrostatic tension could be used as the third mechanical test, but this loading condition is particularly difficult to carry out; the uniaxial tension test (point 3), much easier to perform, is a good alternative.

The behaviour of foams depends generally on their density and the strain rate [13,14]. The yield surface must consequently be characterised as a function of these two variables. Polypropylene foam is employed for energy absorption during crashes (in car bumpers, sports helmets...) where the strain rates may exceed  $100 \text{ s}^{-1}$ . To characterise the foam behaviour at high strain rates, new dynamic devices have to be developed. The first part of this study presented in this paper characterises polypropylene foam

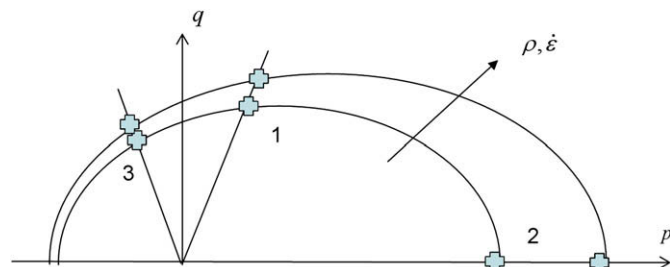


Fig. 2. Yield surface of foam model in hydrostatic deviatoric stress plane.

behaviour under hydrostatic compression at strain rates of  $100 \text{ s}^{-1}$ . For this purpose, a flywheel-driven dynamic testing machine was modified to carry out compression and a hydrostatic chamber was designed to apply pressure on a foam sample at high strain rates.

Hydrostatic compression tests are used in powder metallurgy and soil mechanics research, at low strain rates. Deshpande and Fleck used a hydrostatic compression device on metal foams [8] under quasi-static conditions and Zhang et al. [5] characterised polymer foams under hydrostatic compression for volumetric strain rates less than  $10 \text{ s}^{-1}$  but few researchers have used higher strain rates; Masso, Moreu and Mills [18] studied low density polymeric foams of densities lower than  $50 \text{ kg/m}^3$ , applying the hydrostatic pressure with compressed air in a test chamber. Our objective is to characterise higher density foams under dynamic compression. The apparatus design is based on Deshpande and Fleck's hydrostatic compression device (with pressure applied by a liquid), but imposing higher strain rates. The apparatus was specially developed to allow the measurement of the axial and radial strains of a cylindrical sample; one objective was to reveal the complex deformation of the material under dynamic loading. Initial results on polypropylene foams under uniaxial compression had shown the localisation of deformation of the microstructure of these foams [15]. This paper focuses on the improvement of the dynamic apparatus, and initial results for hydrostatic compression. The paper is organized as follows: Section 2 details the flywheel apparatus and hydrostatic chamber, and the development of an Image Processing Technique (IPT). Section 3 presents results of hydrostatic compression in quasi-static and dynamic conditions; the effects of density and strain rate on the foam behaviour are outlined in Section 4.

## 2. Apparatus

The compression tests on polypropylene foam were carried out on two machines, an electromechanical tension-compression machine and one driven by a flywheel (Fig. 3). One of the objectives of this study was to determine the effect of strain rate on foam behaviour. The first machine was used to characterise the foam response of the material at a low strain rate, and the flywheel at an intermediate strain rate.

Quasi-static compression tests were performed, using a Zwick electromechanical machine with force capacity 250 kN and maximum crosshead velocity 600 mm/min. A force sensor of 10 kN range was used. The displacement imposed on the specimen equalled the crosshead displacement, since the rigidity of the machine is infinite in comparison with the stiffness of the foam specimen.

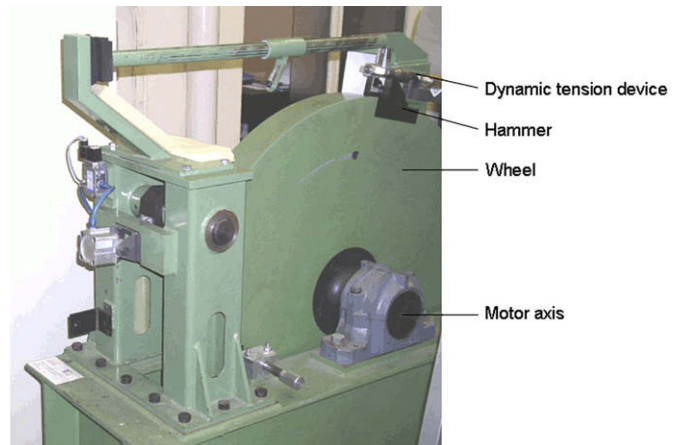


Fig. 3. Picture of flywheel.

## 2.1. Flywheel

The flywheel impact machine is normally used for dynamic tension tests [17]. A steel wheel of diameter 1 m, mass: 617 kg, moment of inertia:  $77 \text{ kg m}^2$  was driven by an asynchronous motor which accurately controls the rotation speed (Fig. 3). A mechanical module had been developed previously to perform dynamic compression tests on polymer foams [13]. This device was modified to improve the measurements of force and specimen deformation during dynamic compression. Propagation of a shock wave during the dynamic loading introduced artefacts in the force response. Changes to the apparatus attenuated this wave, improving the quality of the measurements.

This apparatus is made up of two modules (Fig. 4). Two punches in the first module compress the sample. The fixed upper punch is rigidly fastened to two guide bars, while the lower punch slides along these bars. When the pre-set rotation velocity is reached, an optical sensor detects the position of the hammer, triggering a pneumatic jack which pushes the anvil, attached to a lever, against the wheel. The anvil is then struck by the hammer (point A, Fig. 4). The impact rotates the lever and moves the bar BC, hence the lower punch, vertically upwards (Fig. 5a,b), compressing the sample.

The uniaxial compression of a foam sample is stopped at a pre-set force for two main reasons: the unloaded specimen can be observed after the test to identify damage mechanisms, and the compression force must be limited to avoid damage to the apparatus. Therefore, a mild steel bar BC is installed between the lever and the lower punch. When a pre-determined maximum compression force  $F_m$  is reached, the bar BC buckles, allowing the lever to rotate until the anvil is free of the hammer (Fig. 5c). The length  $L$  and the section of the steel bar BC were calculated using Euler's buckling equation, so  $F_m$  was close to 5 kN:

$$F_m = \frac{\pi^2 EI}{L^2} \quad (1)$$

where  $E$  is the Young modulus of the steel and  $I$  the second moment of area of the bar section.

The compressive force is measured by a Kistler piezoelectric sensor (model 9011A, force range 15 kN, natural frequency 65 kHz) was fastened between the rigid crosshead and the upper punch. The displacement of the lower punch – and thus the deformation of the sample – is measured by a laser displacement sensor. The compression apparatus was designed to perform tests on large size specimens, with a displacement sensor range of 100 mm. For this study, a laser sensor (model OptoNCDT LD 1607-20 from Micro-Epsilon Society) had a 20 mm range. Its linearity is  $200 \mu\text{m}$  and its

cutoff frequency is 37 kHz. The signals from these two sensors are recorded with a National Instrument acquisition card at frequency 100 kHz. These signals allow the evaluation of the compressive force and the punch displacement as a function of time. For uniaxial compression tests, the stress and strain of the sample can be calculated from this data. In the first version of the apparatus, initial test results contained artefacts unrelated to the foam response. An analysis of the dynamic structural response of the testing machine was performed; a Bruel and Kjaer accelerometer was fastened on the lower compression punch and impacts performed with an instrumented hammer (with a piezoelectric force sensor PCB). The transfer function of the device showed resonance frequencies of  $\sim 3$  and  $\sim 6$  kHz. Consequently, it was decided to increase the rigidity of the compression device. Moreover, the steel crosspiece and the lower punch were filled with epoxy hollow spheres (from Ateca S.A.) to reduce their vibration. The wave generated by the impact of the hammer on the anvil was dissipated and attenuated by redesign of the apparatus. First, the contact at point B between the beam BC and the crosspiece is reduced to a segment to increase the change of the mechanical impedance of the point B. This causes the shock wave to be mainly reflected in the crosspiece. The contact between the bar BC and the lower punch is identical, and the variation of impedance in this point C induces again a reflection of the residual wave. The residual shock wave energy is dissipated further in the lower punch, reinforced with the hollow sphere material. With these modifications, only frequencies lower than 2 kHz were transmitted to the lower punch. The transfer function of the compression module shows that the device acts as a low-pass filter.

To conclude, the sample deformation is mainly imposed by the kinematics of the device and not by shock wave propagation (unlike Hopkinson bars, where the wave generated by impact is guided along the input bar to load the sample [13]). The design changes made it possible to dissipate high frequencies and reduce significantly the wave effect on the measurements.

## 2.2. Hydrostatic box

The second device developed for this study is a hydrostatic chamber (Fig. 6), consisting of an aluminium box holding a liquid (alcohol or water) and a steel punch (diameter  $d_p = 20 \text{ mm}$ ). The sample deformation is visible through three glass windows fastened to the aluminium box frame. On the fourth face of this box, a pressure sensor is fastened on a square metallic plate.

Before the test, the sample is placed inside the hydrostatic box, mounted on a pin; air bubbles are carefully eliminated (they

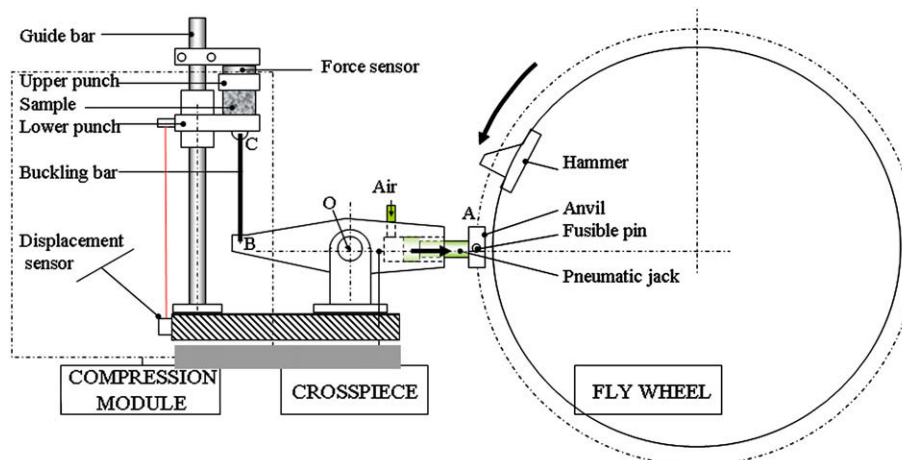


Fig. 4. Scheme of the compression module on flywheel.



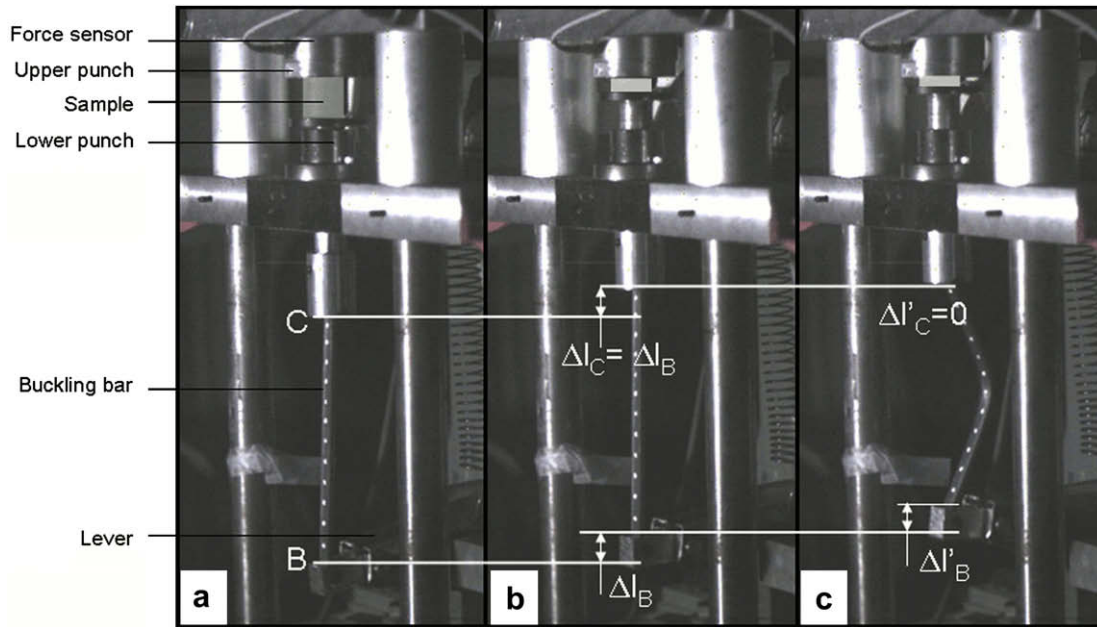


Fig. 5. Three images extracted from a film recorded during a dynamic uniaxial compression tests: a) at the beginning of the test, b) at the end of the compression, c) at the end of the test during buckling of the bar.

would significantly influence measurements of the sample volume). During hydrostatic compression, the punch displacement causes a volume change  $\Delta V$  which is imposed on the foam sample, the liquid and the chamber. To correct for the volume changes in last two of these, calibration tests were performed using a rigid metallic sample, measuring the apparent change in box volume  $V_{\text{box}}(P)$  as a function of the measured pressure  $P$ . This quantity is subtracted from the volume change  $\Delta V$  (at the

same pressure) calculated from the punch displacement, to give the foam volume change.

The volumetric strain  $\varepsilon_v$  of the sample is then calculated from the measurement of the punch displacement  $\Delta h(t)$ , its diameter  $d_p$ , the volume change  $V_{\text{box}}(P)$  and the initial volume  $V_0$  of the sample:

$$\varepsilon_v = \frac{\Delta V}{V_0} = \left[ \frac{\pi d_p^2}{4} \Delta h(t) - V_{\text{box}}(P) \right] \frac{1}{V_0} \quad (2)$$

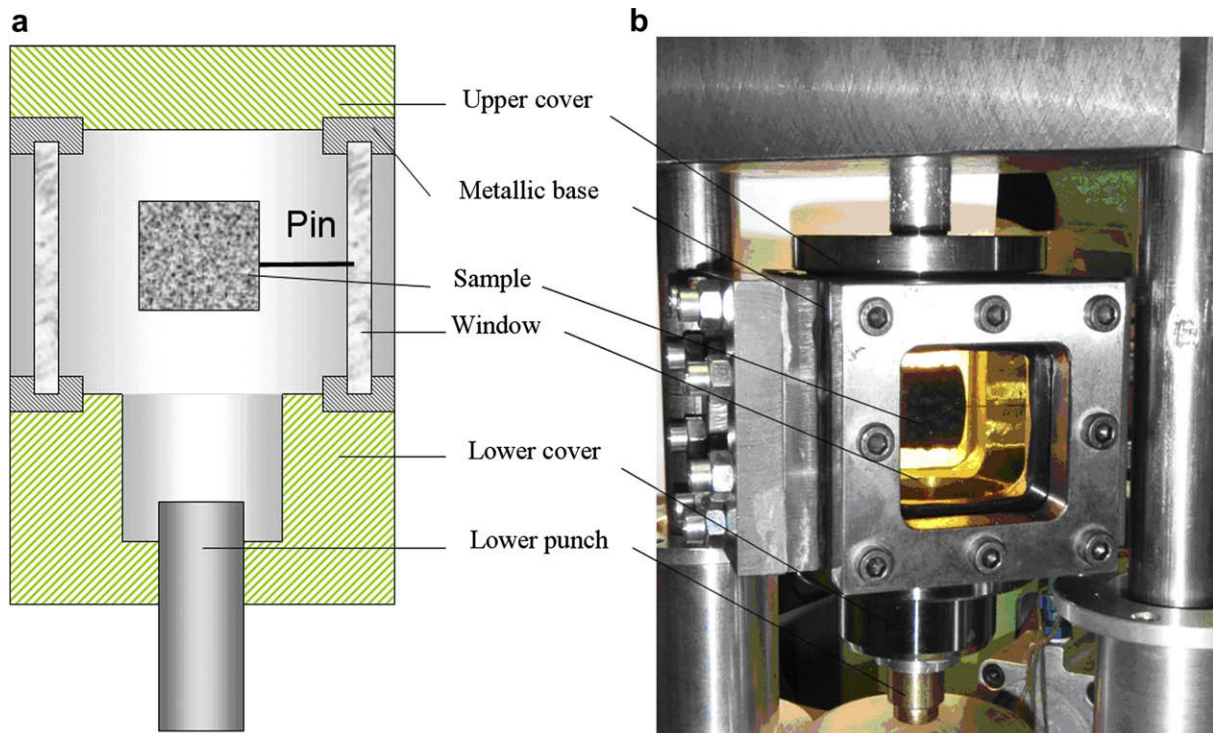


Fig. 6. a) Scheme of the hydrostatic chamber, b) hydrostatic chamber placed in the compression module of the flywheel.

The pressure  $P$  (or the hydrostatic stress) in the chamber is due to the reaction of the sample; during the test, a sample volume change is imposed, and, the higher the sample rigidity, the higher the pressure produced. The chamber pressure is measured with a piezoelectric pressure sensor (Kistler, model 7005, range 60 MPa, natural frequency of 70 kHz) fastened on a steel window of the hydrostatic chamber. The amplified output of this sensor was set to 6 bar per volt. The use of a single sensor supposes that the pressure is uniform in the chamber. This hypothesis is realistic for quasi-static tests but needs to be verified for dynamic hydrostatic compressions.

For high strain rates, the flywheel produced a punch velocity close to 2 m/s. At this velocity, the punch displacement cannot induce pressure waves in the liquid and the wave generated by the impact of the wheel hammer on the anvil is principally dissipated in the crosspiece and not transmitted to the compression punch. To verify the hypothesis of uniform pressure in the chamber, preliminary tests were done, measuring the pressure at several points; quartz windows were replaced with Plexiglas windows instrumented by strain gauges. During the dynamic tests, the deformation of the Plexiglas windows was measured. The gauges were connected to a Vishay conditioning amplifier system (model 2200) with a full-power band pass of 100 KHz. The results (Fig. 7) showed that the pressure measured by the piezoelectric sensor and the pressures deduced from the gauge signals were very close. Therefore the pressure distribution in the chamber was uniform during dynamic hydrostatic compression.

A Photron APX RS3000 high speed camera was used to film the sample deformation during dynamic loading. The pictures were used to determine the volumetric strain of the sample as a function of time, using image processing technique. An acquisition module of the camera recorded the pressure sensor signal during video acquisition. The chamber pressure was therefore known for each image of the deformed sample, during quasi-static and dynamic tests (Fig. 10a).

This hydrostatic compression device can be placed between the jaws of a classical testing machine to characterise the foam behaviour at low strain rates. For higher strain rates, the chamber was placed on the compression apparatus of the flywheel (Fig. 6b).

### 2.2.1. Preliminary tests and device improvement

Initial hydrostatic compressions were done under quasi-static conditions on polypropylene foam of density  $75 \text{ kg/m}^3$ . This foam contains porous beads which are fused together during the



Fig. 7. Pressure (measured by piezoelectric sensor and obtained by gages) in the hydrostatic chamber as a function of punch displacement of the flywheel. This dynamic test was done with a rigid metallic sample.

manufacturing process. Each bead is made of thousands of cells. After this first series of tests, it was seen that the pressurisation liquid penetrated the sample. It was necessary to coat the specimen with a fine tight skin. A silicone gel seems to be the most efficient material to protect the specimen (Fig. 8). The mean thickness of the silicone skin was 0.5 mm and its curing time was been reduced to 10 h to obtain a sufficiently flexible layer (the time recommended by the manufacturer is 24 h), allowing the free deformation of the sample and minimum skin stresses. Hydrostatic compressions carried out on polypropylene foam with silicone protection confirmed its water tightness.

To characterise the viscoelasto-plastic behaviour of polymeric foams, liquid pressure and punch displacement must be measured accurately to determine stress versus volumetric strain. The pressure is recorded with a sufficient accuracy using the piezoelectric pressure sensor, so complementary techniques must be developed to measure volumetric strain. The calculation of the volumetric strain requires the punch displacement measurement and the determination of the variation of the chamber volume  $V_{\text{box}}$  (equation (2)). The punch displacement is accurately obtained from the displacement sensor of the Zwick machine during static compression, or with a laser sensor on the flywheel during dynamic loading. However, the chamber volume variation  $V_{\text{box}}$  is difficult to measure accurately because the rigidity of the chamber is not a linear function of the chamber pressure  $P$  (Fig. 7) and depends on several variables. The chamber rigidity depends on the non-linear stiffness of rubber gaskets placed between glass windows and the frame. The deformation of rubber located between the punch and the chamber, and small air bubbles (left in the chamber after sample introduction) also influence the rigidity of the chamber.

Due to this uncertainty, the variation of the volumetric strain can be only determined coarsely from the punch displacement, so other methods had to be developed. Because classical devices such as gages or extensometers cannot be used, a non-contact measurement method based on image processing was developed to measure more accurately the volumetric strain.

Each hydrostatic compression test was filmed to determine the volumetric strain of the specimen, and to reveal any localisation of sample deformation at high volumetric strain. The image definition is crucial, since the images were analysed to determine the diameter and the height of the specimen. With the Photron APX RS3000 high speed camera, the image resolution depends on the video acquisition frequency. This frequency was chosen as a function of the volumetric strain rate imposed on the sample; for quasi-static tests, the frequency was 50 frames per second (resolution  $1024 \times 1024$  pixels), for dynamic tests it was 10 000 frames per second with a resolution of  $512 \times 512$  pixels. The time between two images was 20 ms and 0.1 ms respectively for quasi-static and dynamic tests, but the shutter time was reduced to 1 ms for quasi-static tests and  $50 \mu\text{s}$  for dynamic compressions to minimize the variation of the volumetric strain during image capture; this was  $16 \times 10^{-6}$  and  $25 \times 10^{-3}$  for quasi-static and dynamic compressions at strain rates of  $16 \times 10^{-3} \text{ s}^{-1}$  and  $50 \text{ s}^{-1}$  respectively. It was not possible to further reduce the shutter time while obtaining good quality images of sufficient contrast.

When the sample was filmed from the side (Fig. 9), its diameter  $d_m$  and height  $h_m$  can be measured directly in pixels. To obtain these two parameters, each image was numerically processed as follows:

1. A rectangular border frame surrounded the sample (Fig. 9a).
2. In this selected area, an intensity threshold was used to produce a black image of the foam sample, ignoring the pin and the silicone skin (Fig. 9b).
3. White pixels inside the sample edge were included (Fig. 9c).

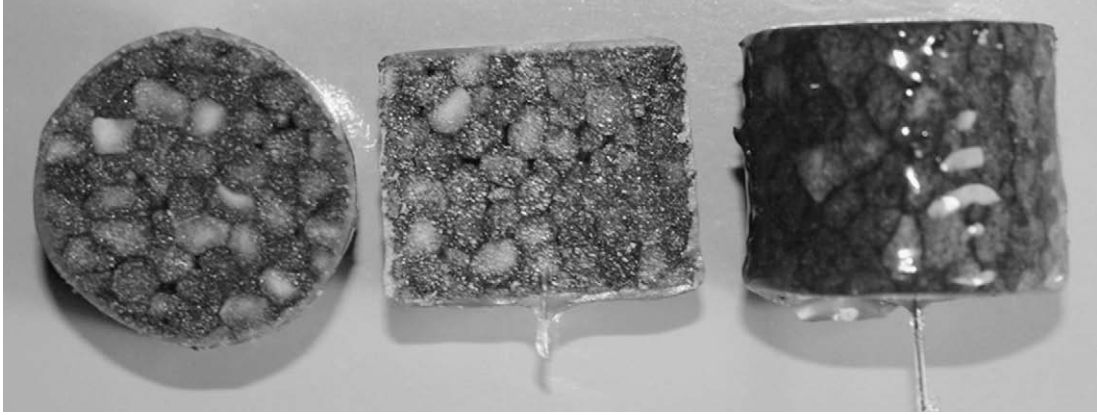


Fig. 8. Polypropylene foam sample with its silicone gel coat.

The mean diameter  $d_m(t)$  and the mean height  $h_m(t)$  are determined, for each image, from the black sample area and the edge perimeter. The volumetric strain was calculated from the equation:

$$\varepsilon_v = \frac{\Delta V}{V_0} = \frac{h_m(t=0)d_m^2(t=0) - h_m(t)d_m^2(t)}{h_m(t=0)d_m^2(t=0)} \quad (3)$$

Use of this equation assumed that the specimen response is isotropic or orthotropic. This hypothesis cannot be verified without the use of another high speed camera to film a different side view. However, hydrostatic compression tests, with the camera axis aligned with the sample axis (Fig. 10b), showed that the deformation of the polypropylene foam cylinder was axisymmetric. Therefore, the use of equation (3) to calculate volumetric strains was justified.

### 3. Material and experimental results

The foams studied were closed cell polypropylene foams manufactured by JSP S.A. This foam consisted of expanded beads fused together. Their mean diameter is about 2 mm and their wall thickness is about 0.1 mm. On a micro scale, the beads contain closed cells with walls which no more than a micron thick. The cell size is relatively homogeneous, with mean diameter of about 0.1 mm (Fig. 11).

The microstructure of expanded polypropylene foams is due to their manufacturing process. The first step consists in the pre-

expansion of small polypropylene granulates into beads of density 30–50 kg/m<sup>3</sup>. These expanded beads are injected into a steam chest mould, where they fuse together under steam heat and pressure: the cell gas expands the beads, which agglomerate and fuse together to form the structure of the foam. The density of each moulded part depends on the number of porous beads injected into the mould. The microstructure of these foams varies with density. The different microstructures, observed by SEM, are shown for densities of 34, 76 and 114 kg/m<sup>3</sup> (Fig. 11).

Cylindrical samples of diameter 25 mm and height 20 mm, of densities from 35 to 114 kg/m<sup>3</sup>, were cut from the centre of large moulded foam blocks (700 mm × 500 × 200 mm) where the density is the most homogeneous. Such samples contain more than 600 beads (see the two sections in Fig. 8), enough to consider the samples as representative. The samples were sanded, measured and weighed. A study showed that the variation of the density inside each sample is low [16]. The same size samples were used for uniaxial compressions [16] and hydrostatic loadings.

#### 3.1. Hydrostatic compression at low strain rates

The initial hydrostatic compression tests were done at low strain rate with the electromechanical testing machine, using a punch displacement rate of 30 mm/min. The initial volumetric strain rate was then  $16 \times 10^{-3} \text{ s}^{-1}$  with a sample of diameter 25 mm and height 20 mm. A typical variation of the stress versus time is plotted Fig. 12 for a foam specimen of density 115 kg/m<sup>3</sup>. The

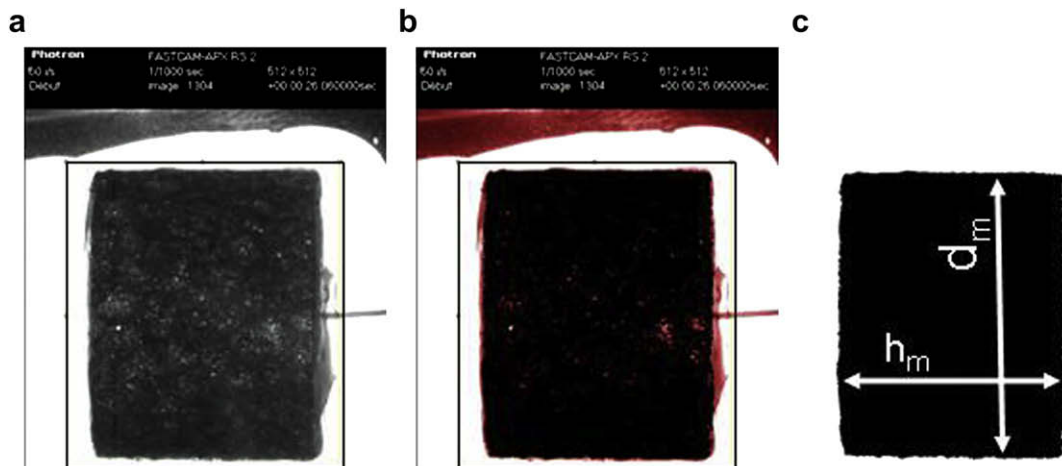
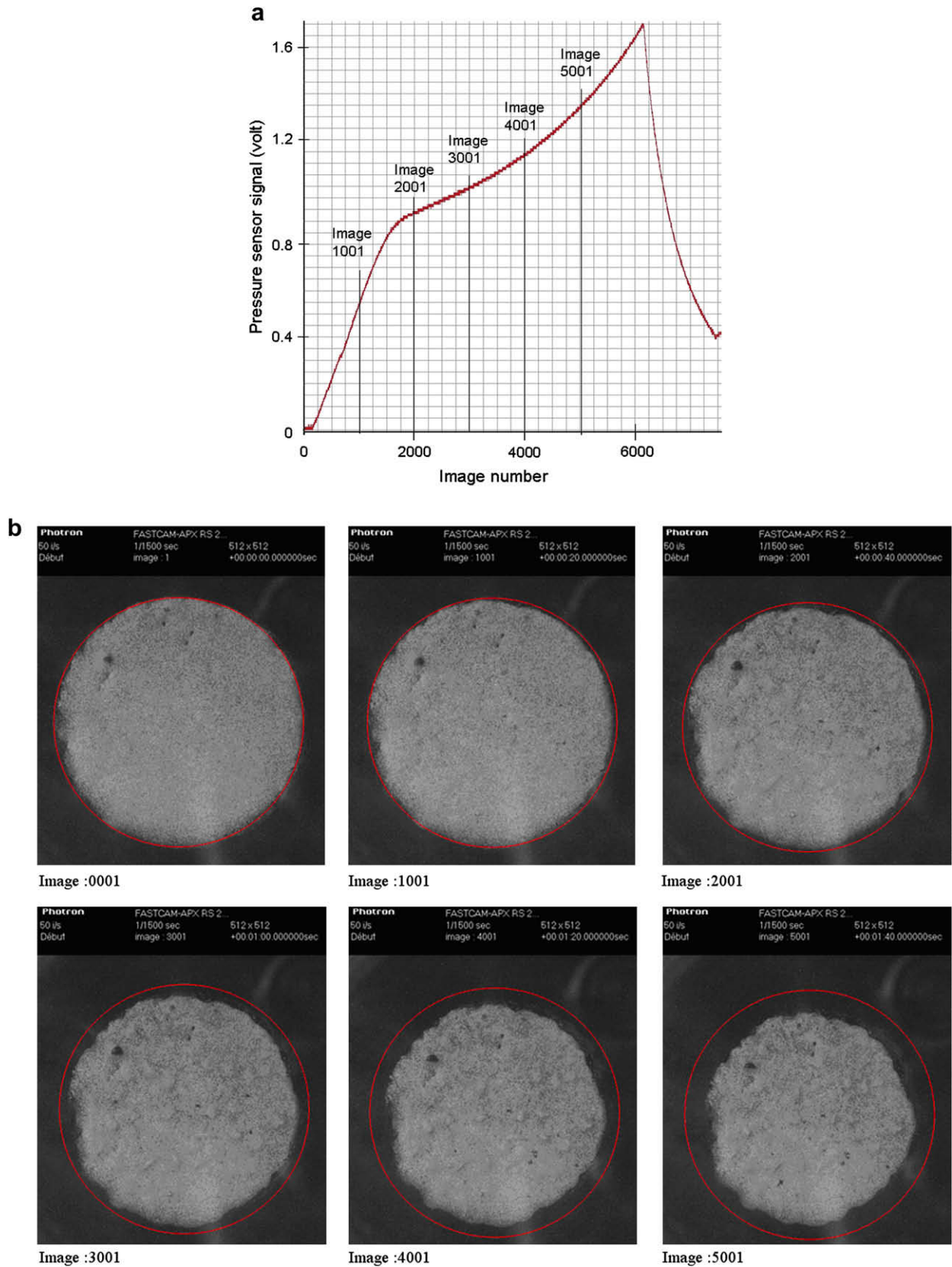


Fig. 9. Filtering of the sample image: a) raw picture, b) threshold of the picture, c) final edge to obtain the diameter and the height of the sample.





**Fig. 10.** a) Stress versus image number recorded by the high speed camera during quasi static hydrostatic compression. b) change of shape of the foam sample (in front view) at 6 times (indicated in (a)) of the quasi static hydrostatic compression.

transition between the elastic behaviour and the plastic plateau is not clear (contrarily to the classical transition observed during uniaxial compression), and the curve concavity reveals a non-linear

elastic behaviour of the polypropylene foam under hydrostatic behaviour. The sample deformation was filmed with the high speed camera, and six pictures (Fig. 13) were extracted (with an interval



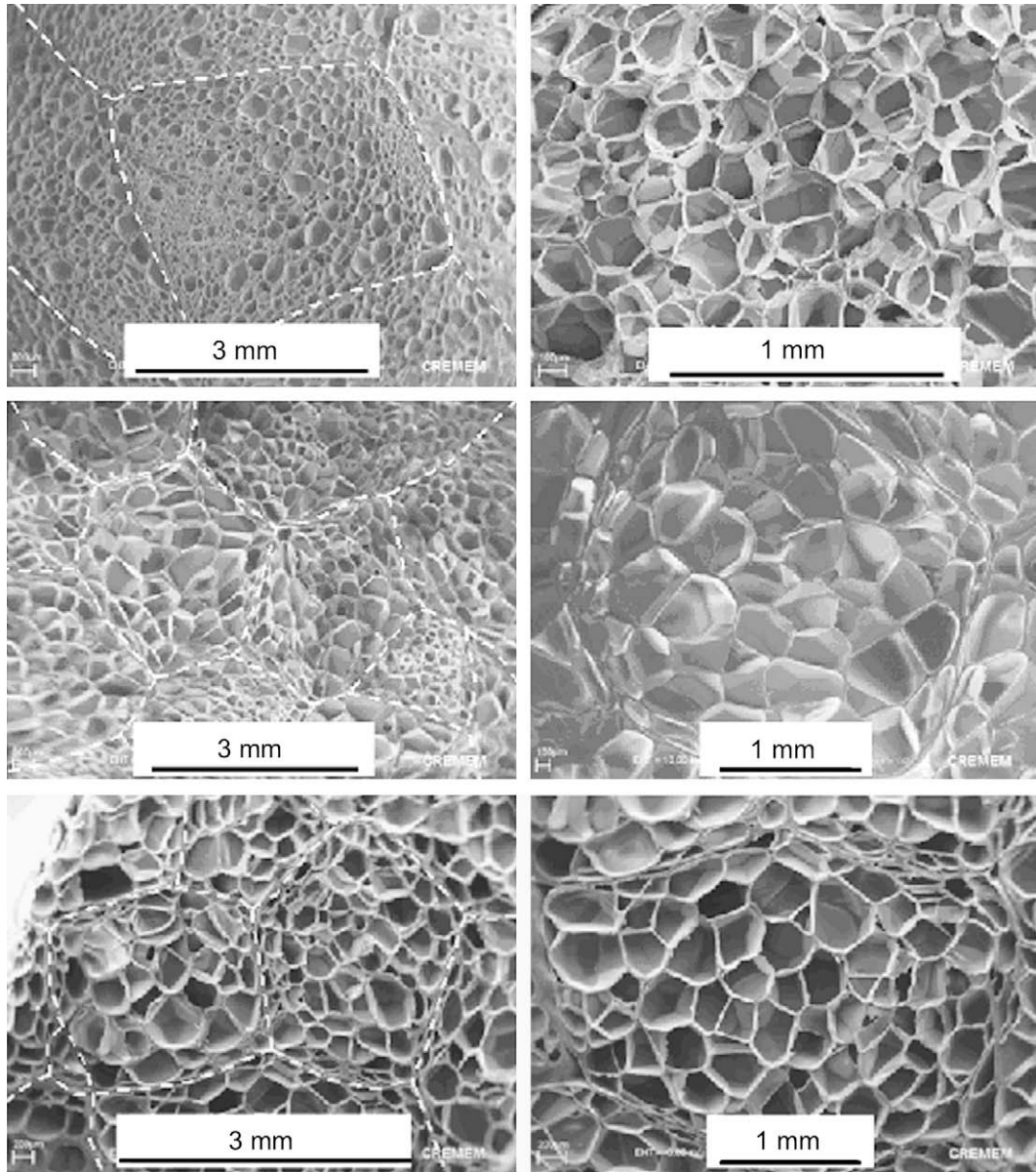


**Fig. 11.** Microstructure of the polypropylene foam for three densities.

time of 5 s, points a–f on Fig. 12) from this film. Fig. 13a shows the initial shape of the sample. The camera view was precisely aligned with the sample axes; the diameter (along the axis  $\vec{e}_r$ ) and the height (along the axis  $\vec{e}_z$ ) were then measured easily. The initial edge of the sample (in red) is also plotted on pictures (Fig. 13b–f) to show the variation of sample shape; this edge is not used to calculate the volumetric strain as a function of time (the pin and silicone skin are removed by image processing). At the beginning of the hydrostatic compression, the change in sample volume is small (Fig. 13b), but can be visually detected. Therefore Image Processing could determine small volumetric strains during the first phase of the behaviour. Although the reduction of diameter is significant, it is difficult to detect any reduction in height. Therefore the sample deformation is not isotropic, a phenomenon detailed in Section 4. The following four pictures (13c–f), recorded during the stress plateau region (points c–f of Fig. 12), reveal significant reductions of the sample volume.

Measurements of pressure and punch displacement, and the image processing results, made it possible to determine the stress

versus volumetric strain behaviour of foams of a range of densities from 35 to 114 kg/m<sup>3</sup> (Figs. 14 and 15). The similar curves are characteristic of foam behaviour: an elastic behaviour is followed by a plastic plateau and finally densification. Fig. 14 compares stress versus volumetric strain data from the punch displacement measurements and image analysis. For most tests, these two methods give similar results and the  $\sigma - \varepsilon_v$  curves are very close. The punch displacement measurements allow volumetric strain to be measured up to densification strains, but the image processing method is more accurate for lower deformation, so this method was chosen to characterise the elastic behaviour and the plastic plateau. The characteristics determined are the slope of the elastic behaviour, the yield stress and the slope of the plastic plateau.

The initial response of this polypropylene foam under hydrostatic compression was non-linear. In uniaxial compression tests on this foam, the stress is a linear function of strain during the first instants of loading, [13] and the foam behaviour can be considered elastic for stresses lower than a yield stress  $\sigma_m$ . A compressibility modulus  $K$  was defined as the initial slope of the curve  $\sigma - \varepsilon_v$ . To

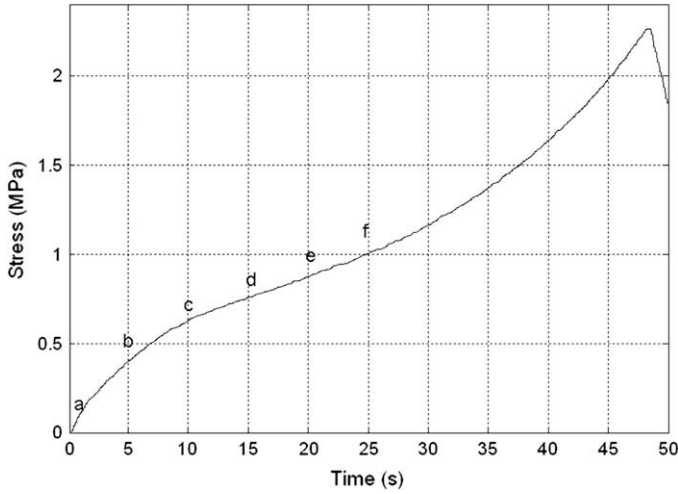


**Fig. 12.** Stress versus time response of a PPE foam of density  $114 \text{ kg/m}^3$  under quasi static hydrostatic compression.

measure  $K$ , the slope of the least-squares line (segment AB, Fig. 15) was calculated from a set of data for volumetric strains lower than an arbitrary value  $\varepsilon_K = \varepsilon_m/4$  with  $\varepsilon_m$  the volumetric strain of the point I ( $\sigma_m, \varepsilon_m$ ) considered as the transition between the elastic behaviour and the plastic plateau. This smooth transition between the elastic and plastic plateau stages is characterised by a yield stress  $\sigma_m$ . The characterisation of the yield stress  $\sigma_m$  is difficult because the initial stress-strain behaviour of the foam exhibits concavity; a tangent method was then chosen to determine  $\sigma_m$ : it is

the stress at the intersection between the initial slope for elastic behaviour (segment AB, Fig. 15) and the tangent to the plastic plateau (segment CD). The point I ( $\sigma_m, \varepsilon_m$ ) is considered to occur at the transition between the elastic and plastic responses. To complete this characterisation, the tangent modulus  $E_T$  is defined as the slope of the plastic plateau. The plastic plateau is non-linear so the tangent modulus  $E_T$  is a function of the volumetric strain. For this initial characterisation of foam behaviour,  $E_T$  was determined from the slope of the least-squares line (segment CD, Fig. 15) for strains  $0.1 < \varepsilon_v < 0.2$ .

The stresses as functions of volumetric strain, obtained by image processing (Fig. 15), show that:

1. An increase in density causes the compressibility modulus  $K$  to increase. A higher foam density involves a greater quantity of polypropylene, either because there are more cells or the cell walls are thicker, so the foam structure is more rigid.
2. The yield stress  $\sigma_m$  increases also as a function of the density, for the same reason.
3. The plastic plateau is non-linear, with a slope that increases with strain. This effect is probably due to the increase of the gas pressure inside the foam cells and the progression of the damage to the more rigid cells (at the beginning of the plastic plateau, the weaker cell walls buckle before the stronger ones).
4. Densification appears at lower volumetric strains for higher densities. The initial void volume fraction is lower for higher densities, and densification appears for lower macroscopic deformation in the case of higher densities when the porosity of the foam tends to zero.

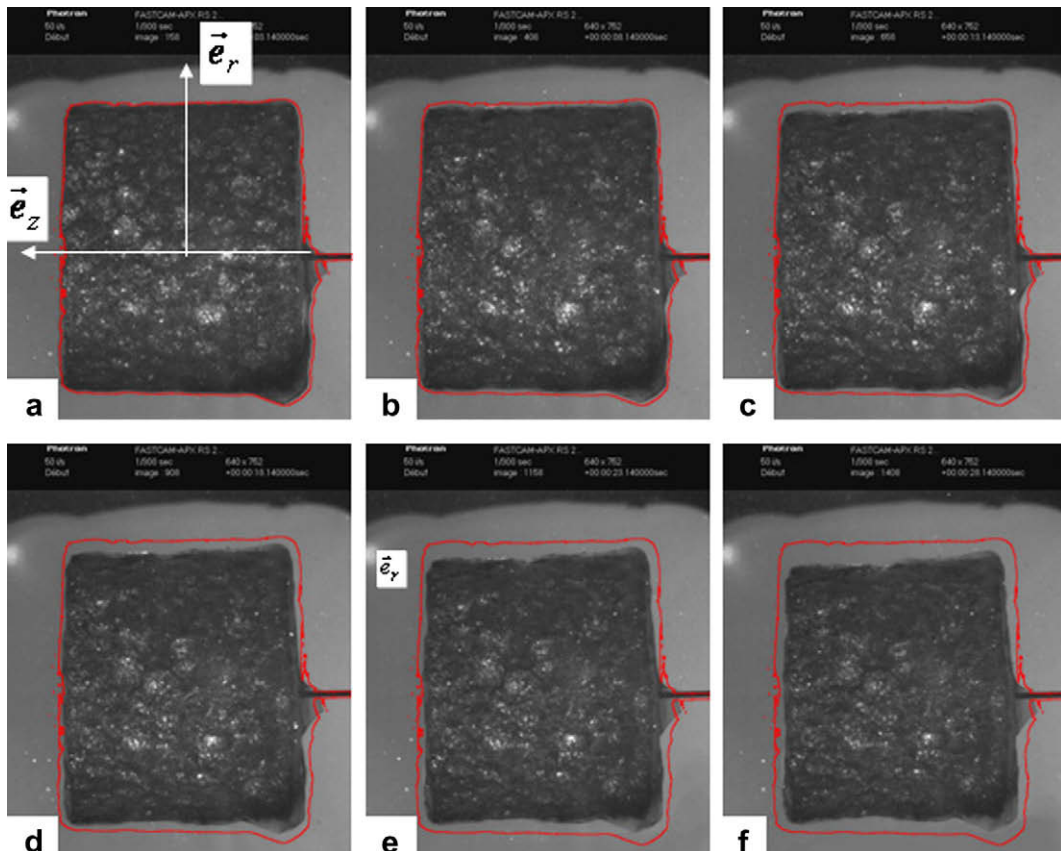


**Fig. 13.** Change of shape of the foam sample (in side view) at 6 times (indicated in Fig. 12) of the quasi static hydrostatic compression.

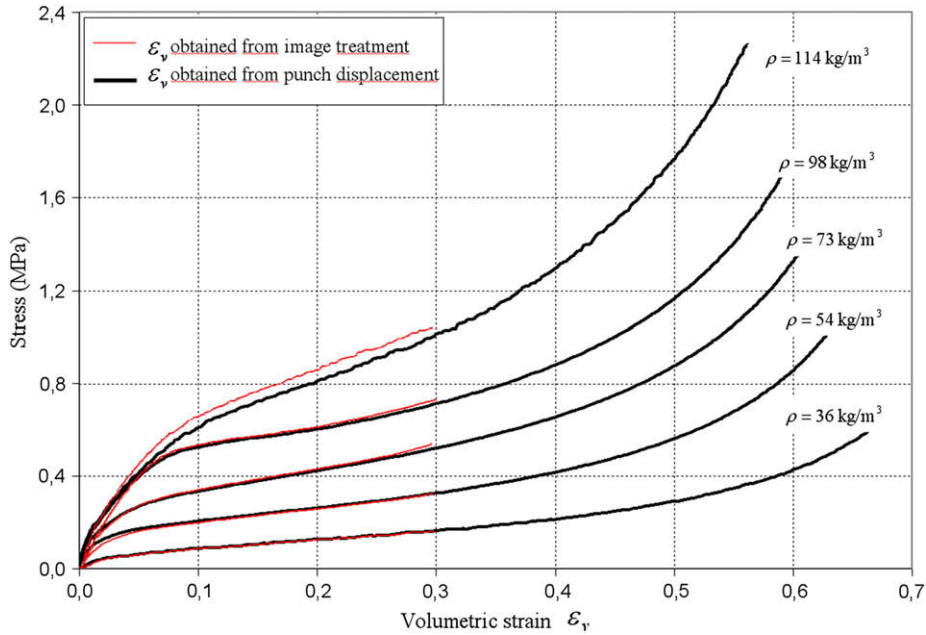


Fig. 14. Stress versus volumetric strain of PPE foam of 5 densities under quasi static hydrostatic compression (the volumetric strain was obtained from displacement punch measurement).

### 3.2. Hydrostatic compression at high strain rates

The hydrostatic compression tests at high strain rate used the hydrostatic chamber driven by the flywheel. A flywheel rotation velocity of 30 RPM caused a punch displacement rate of 1.5 m/s. The initial volumetric strain was  $50 \text{ s}^{-1}$  for a sample of diameter 25 mm and height 20 mm. The sample deformation was also filmed with the high speed camera at a frequency of 10 000 pictures per second, with resolution  $512 \times 512$  pixels. For these tests, two additional spotlights were used to obtain with good contrast images. Six pictures (Fig. 16) were extracted at intervals of 1.2 ms from the film of a test on a  $94 \text{ kg/m}^3$  density foam. The first picture

shows the initial shape of the sample, with its edge outlined in red. The following pictures (15b–f) allow comparisons with the initial shape. In the second picture, taken at the beginning of the plastic plateau (Fig. 15b), the changes in diameter and height are similar whereas the radial strain is larger than the axial strain for higher deformations (Fig. 15c–e).

Six densities were tested: approximately 35, 54, 73, 81, 98 and  $120 \text{ kg/m}^3$ . The curves of the stress versus volumetric strain obtained from the punch displacement measurement and the image processing are close (Fig. 17). It has been shown that the results deduced from punch displacement measurement are less accurate for lower deformation and the image processing method

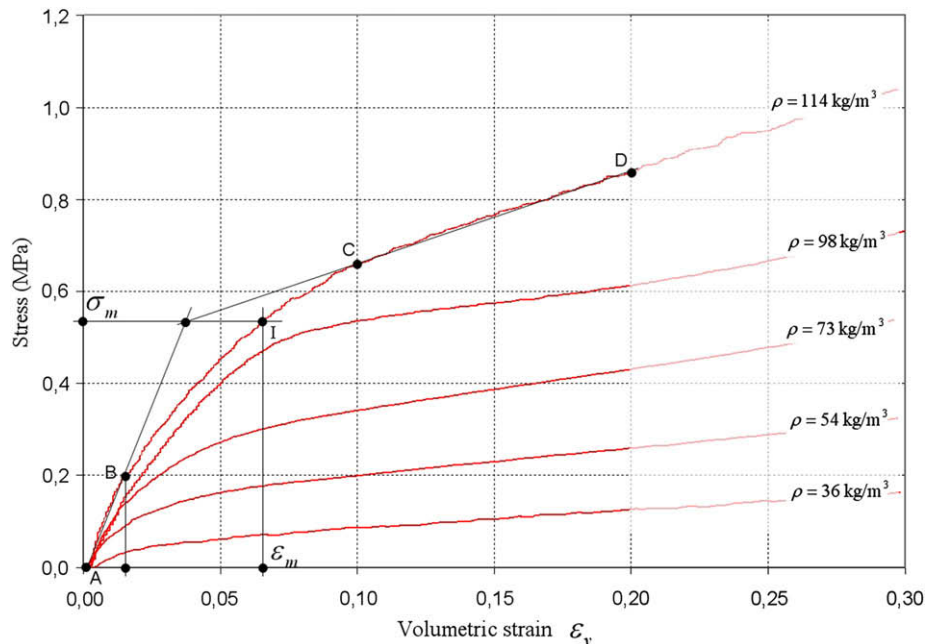


Fig. 15. Stress versus volumetric strain of PPE foam of 5 densities under quasi static hydrostatic compression (the volumetric strain was obtained from image processing technique).



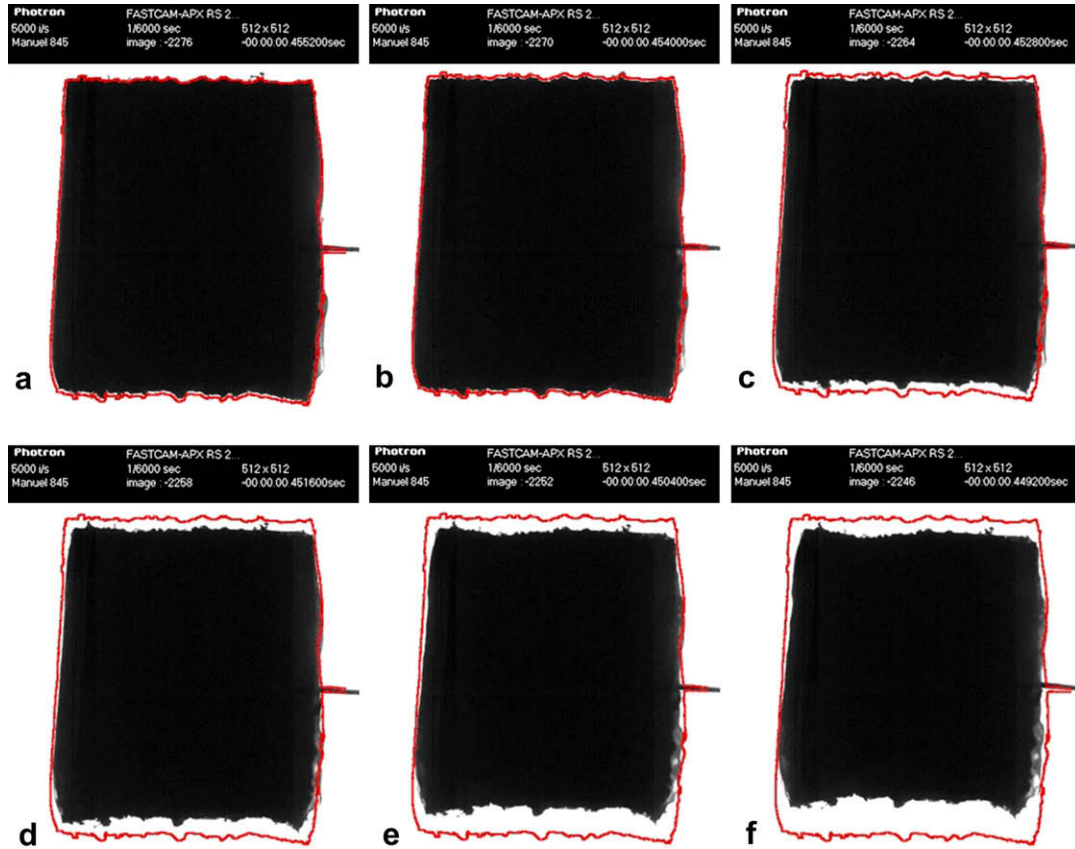


Fig. 16. Change of shape of the foam sample at 6 times of the dynamic hydrostatic compression (a/initial shape, 1.2 ms between two images).

has been chosen to identify the foam behaviour. However, image processing produced less volumetric strain measurements than for static loadings (Fig. 18): At high strain rates, the yield stress is reached in less than 2 ms (depending on the foam density) and only 20 volumetric strain measurements can be determined by image processing. The 10 000 frames per second frequency of the high speed camera produced the best combination of number of measurement points and image resolution.

In spite of this lower accuracy, the foam behaviour was characterised by the compressibility modulus  $K$ , the yield stress and the

tangent modulus, using the same method as for quasi-static results. This revealed:

1. During the first step of the dynamic compression (Fig. 18), the stress–strain curve is less concave than for quasi-static results. The foam density affects the compressibility modulus  $K$ .
2. The yield stress increases as a function of the density, and is greater than that determined at lower strain rates.
3. The tangent modulus  $E_T$  increases as a function of density. However, the value of  $E_T$  obtained for foam density  $98 \text{ kg/m}^3$  is

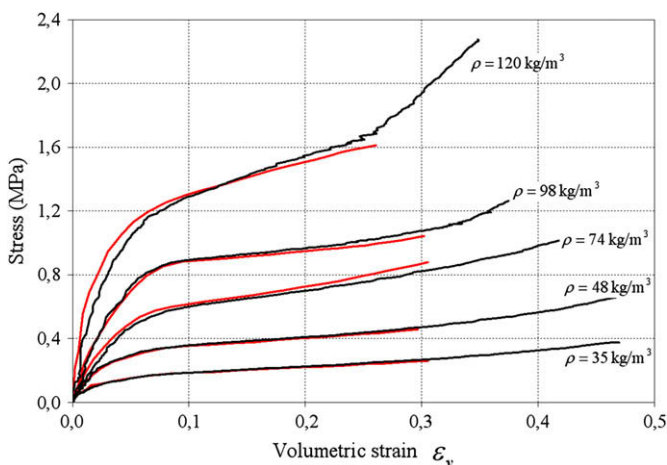


Fig. 17. Stress versus volumetric strain of PPE foam of 5 densities under dynamic hydrostatic compression (the volumetric strain was obtained from displacement punch measurement).

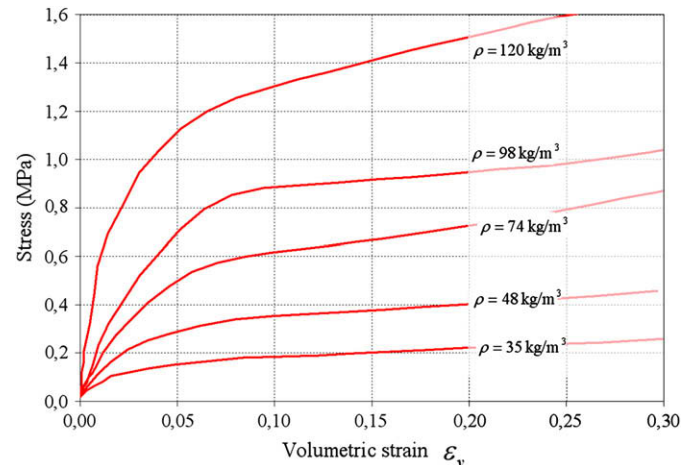


Fig. 18. Stress versus volumetric strain of PPE foam of 5 densities under quasi static hydrostatic compression (the volumetric strain was obtained from image processing technique).



close to the one calculated for the lower  $73 \text{ kg/m}^3$  density. This result was confirmed by several tests.

4. Densification strains were not reached for foam densities lower than  $98 \text{ kg/m}^3$  (the displacement of the punch was limited to reduce the maximum pressure applied in the chamber and avoid apparatus damage).

#### 4. Discussion

More than 100 hydrostatic compressions tests were done to develop the apparatus, to validate the image processing method, and to verify the hypotheses of uniform chamber pressure and the axisymmetric deformation of the polypropylene foam. 40 hydrostatic compression tests were done on polypropylene foam of densities from  $35$  to  $120 \text{ kg/m}^3$  to characterise the foam behaviour in quasi static and at high strain rate close to  $50 \text{ s}^{-1}$ . For each strain rate, the influence of the density on the stress response has been demonstrated. Three parameters were determined, that constitute a database for characterising mechanical models of the foam behaviour. These parameters are the compressibility modulus  $K$ , the yield stress  $\sigma_m$  and the plastic plateau slope or tangent modulus  $E_T$ .

##### 4.1. Viscoelastic behaviour

It is particularly delicate to characterise the viscoelastic behaviour of cellular material as a function of the strain rate. For the first time, this new apparatus of hydrostatic compression coupled with an image processing technique has been used to estimate the compressibility modulus  $K$ . Fig. 19a shows that the dispersion of results is lower for quasi-static tests than for high strain rate tests. For lower densities, the dispersion is less than  $1 \text{ MPa}$  (for quasi-static tests) and increases with the density. It reaches  $5 \text{ MPa}$  for a density of  $120 \text{ kg/m}^3$  for each strain rate.

In spite of this dispersion, the compressibility modulus  $K$  was an increasing function of density for each strain rate (Fig. 19a). Furthermore, it is a linear function of density for each strain rate condition. The influence of the strain rate on this parameter is particularly significant for the higher density foam, and shows the viscosity of the polypropylene foam under hydrostatic compression.

The behaviour of the polypropylene is non-linear under hydrostatic compression (the stress-strain curve is initially concave) whereas the stress response of this same foam is a linear function of strain under quasi-static or dynamic uniaxial compressions [16]. It seems that the non-linear behaviour of this foam is only revealed under hydrostatic loading. In order to better understand the non-linearity of the stress-strain response, the physical phenomena that occur in the foam microstructure should be considered. This foam is a two-phase material, consisting of beads, cells and a gas. Its behaviour can be due to a combination of the behaviour of the solid polypropylene and the viscosity of the gas which flows through the micro-porous walls of beads and cells. During compression, the strain field is non homogeneous; bead density varies, hence their rigidity varies. One can assume the less dense beads are more deformed (the deformation of the foam structure is complex; the shape of the structure and the organization of beads in this structure significantly influence the distribution of bead and cell deformation [17]). The bead volumetric strain, depending on density, varies randomly with position in the foam, inducing a stochastic field of gas pressure. Finally, the gas pressure in the sample tends to become homogeneous since the higher pressure gas (in the more deformed beads) flows through beads and cells to the lower pressure, less-deformed beads. This viscous flow of the gas may involve the non-linearity of the global foam viscoelastic behaviour. This assumed mechanism is specific to the

hydrostatic compression since the gas contained in the foam structure is enclosed in the volume of the deformed sample.

This hypothesis takes into account the effect of the density. For higher densities, the walls of beads and cells are either thicker or their number is larger. The higher the foam density, the more difficult is the gas exchange between beads, and the gas flow is consequently more viscous because of capillarity physics. On the contrary, for lower densities, cell wall thicknesses are lower or their number is less, and the equilibrium of the gas pressure inside the sample is then easier. For these reasons, the strain rate effect does not appear for foam densities close to  $35 \text{ kg/m}^3$ .

In conclusion, this foam has to be considered as a two-phase material – or a complex multi scale structure including a gas flow – to better understand the foam viscoelastic behaviour under hydrostatic compression. The hydrostatic compression test, initially used to characterise the macroscopic behaviour of polymeric foams, can be also considered as a compression test on a complex structure.

##### 4.2. Plastic plateau

Raw data were measured for each density, under the two conditions of strain rate. The plastic plateau (the parameters  $\sigma_m$  and  $E_T$ ) was characterised for each density, at two strain rates (Fig. 19b,c). The dispersion of the yield stress was close to  $0.1 \text{ MPa}$  and seems independent of density and strain rate. The dispersion of the tangent modulus  $E_T$  was low for lower density foams ( $0.1 \text{ MPa}$  for density  $35 \text{ kg/m}^3$ ) and increased as a function of the density, becoming  $0.5 \text{ MPa}$  at density  $98 \text{ kg/m}^3$ .

The variations of  $\sigma_m$  and  $E_T$  with density (Fig. 19b,c) show:

1. The yield stress increases as a linear function of density for each strain rate. The effect of the velocity is obvious in Fig. 19b, and this influence increases with density. The strain rate dependency of the solid polypropylene is well known. As a consequence, the sensitivity of the foam yield stress to strain rate is greater for foams of higher densities.
2. The tangent modulus  $E_T$  increases with the foam density, even if the behaviour of the foam of density  $98 \text{ kg/m}^3$  is peculiar. For low densities, the variation of  $E_T$  is a linear function of density (Fig. 19c). It increases strongly for densities higher than  $110 \text{ kg/m}^3$ . The singular response of foam of density  $98 \text{ kg/m}^3$  has been confirmed from several tests and appears at the two strain rates. Its microstructure and its chemical composition were analysed, and found to be typical for such foams. Moreover, the strain rate has no effect on the tangent modulus. Under hydrostatic compression, the effect of the gas under pressure is significant and one can assume the distribution of the gas pressure became homogeneous during the previous non-linear elastic phase. Therefore, the viscous effect of the gas flow is less during the beginning of the plastic plateau (where the tangent modulus was measured).

##### 4.3. Anisotropy and strain localisation

The hydrostatic compression apparatus allowed measurements of sample deformation with a high speed camera. The variations of the mean diameter  $d_m$  and the mean height  $h_m$  of the sample were measured to obtain the volumetric strain. These results were also used to calculate the radial and axial strains. The axial strain  $\varepsilon_z$  as a function of time is calculated as the ratio between the variation of the height  $\Delta h_m(t)$  of the sample and its initial height  $h_m(t=0)$ :

$$\varepsilon_z = \frac{\Delta h}{h_0} = \frac{h_m(t=0) - h_m(t)}{h_m(t=0)} \quad (4)$$

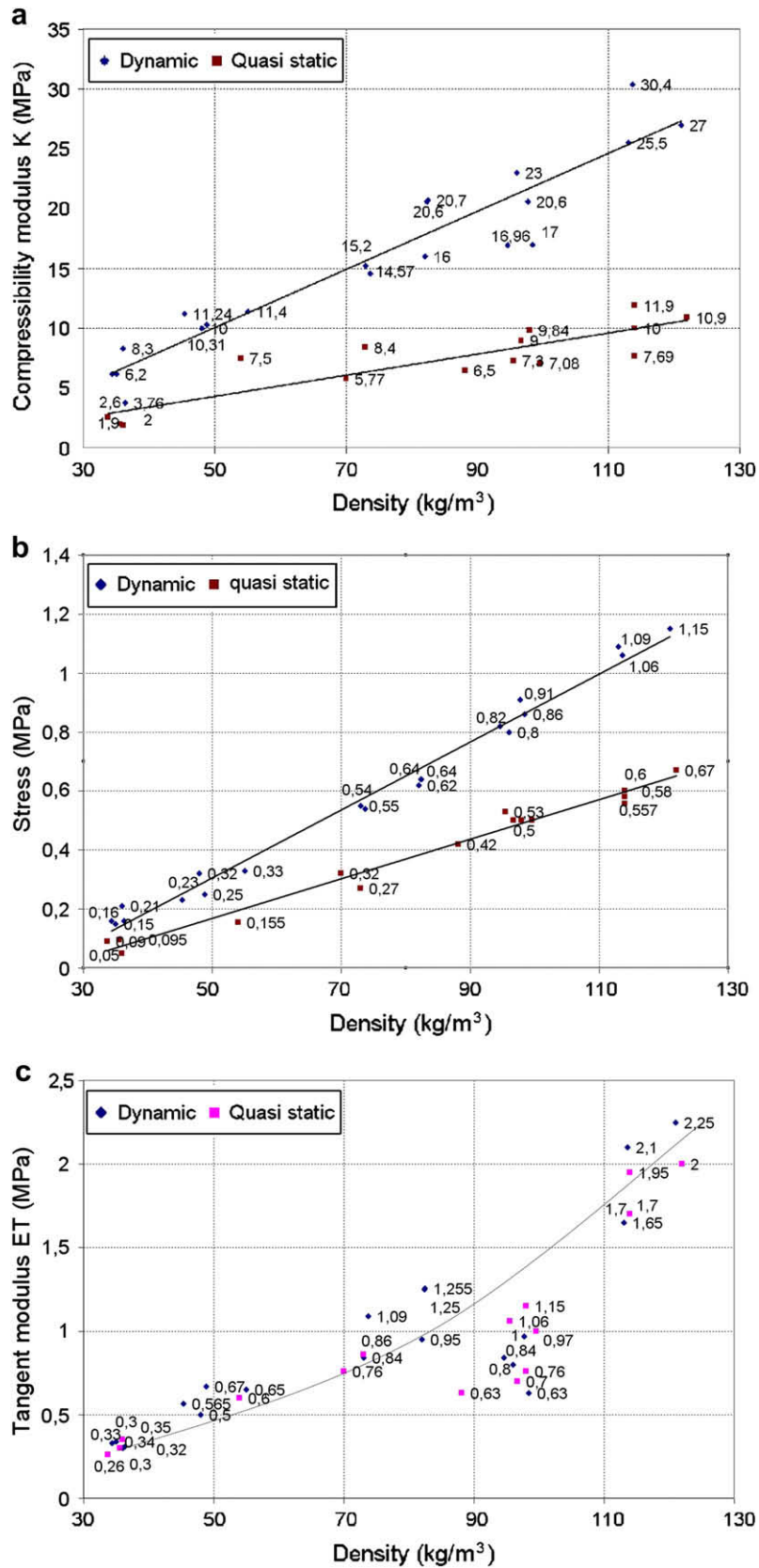


**Fig. 19.** a) Variation of the compressibility modulus as a function of the density for two strain rates. b) variation of the yield stress as a function of the density for two strain rates. c) variation of the tangent modulus as a function of the density for two strain rates.

The mean heights  $h_m(t)$  and  $h_m(t=0)$  are in pixels (obtained directly by image processing) but the calculation of the axial strain does not require any conversion of units. The radial strain is obtained by a similar equation, from the variation in sample diameter  $d_m$ :

$$\varepsilon_r = \frac{\Delta d}{d_0} = \frac{d_m(t=0) - d_m(t)}{d_m(t=0)} \quad (5)$$

The images of hydrostatically compressed samples under quasi static (Fig. 13) or high strain rate (Fig. 16) conditions showed that the diameter changed more than the height. Fig. 20a (showing the typical variation of the axial strain as a function of the radial strain for several densities) highlights that the axial strain  $\varepsilon_z$  was smaller than the radial strain  $\varepsilon_r$  (except for the density  $114 \text{ kg/m}^3$  where the strains are similar). The axial strain  $\varepsilon_z$  is particularly low compared to the radial strain  $\varepsilon_r$  during the viscoelastic behaviour and becomes more significant during the plastic plateau. The sample deformation was already shown to be axisymmetric; one can also note that the change of diameter is more significant. Therefore, the behaviour of polypropylene foam seems transversely isotropic under hydrostatic compression.

As a first approach, one can consider that the variation of the axial strain is a linear function of the radial strain, so the transverse strain isotropy can be characterised by the ratio  $K_r = \varepsilon_z/\varepsilon_r$ . This ratio was calculated for each hydrostatic compression test, to evaluate the influence of the density on the transversely isotropic behaviour of the foam. It is difficult to establish a tendency of this ratio  $K_r$  as

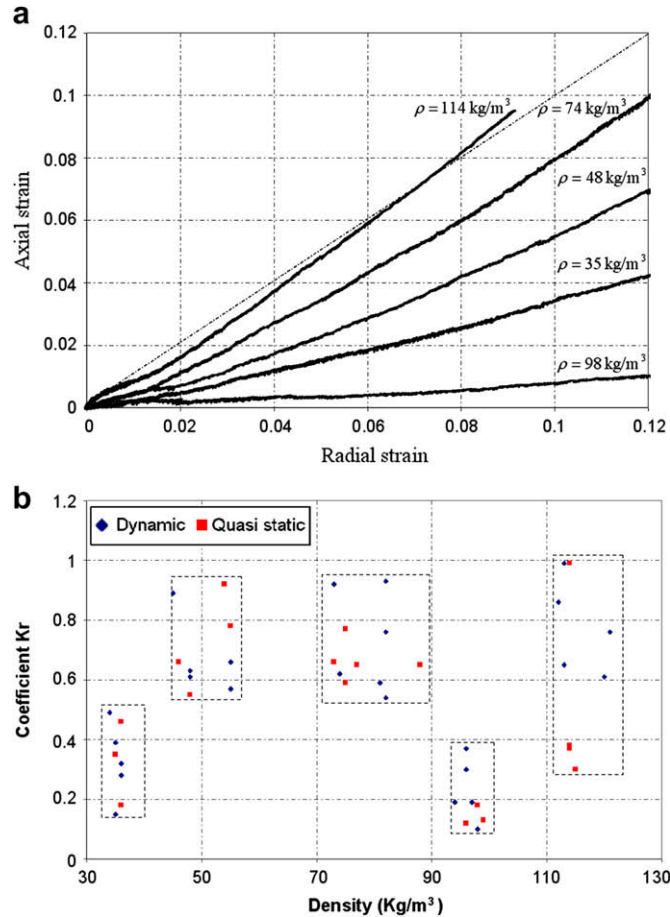


Fig. 20. a) Axial strain versus radial strain of foam samples under quasi static hydrostatic compression for 5 densities and showing the anisotropy of the deformation. b) variation of the ratio  $K_r$  as a function of the density for two strain rates.

a function of the density (Fig. 20b). However, for each density, 35, 50, 80, 96 and  $114 \text{ kg/m}^3$ , one can estimate a mean value for the ratio  $K_r$  (even if the dispersion of the result is significant for each density). It is probable that the ratio  $K_r$  is related to the foam block from which the samples were extracted. In other terms, one can suspect an effect of the process on the microstructure of the foam and in consequence on the apparent anisotropy of the material revealed by the ratio  $K_r$ . Moreover, for each density, the significant dispersion of the ratio  $K_r$  can be explained in considering the propagation of the damage at the scale of the microstructure. It was already shown that, for this kind of polymeric foam under uniaxial compression, the buckling of the cell and bead walls appears firstly on the weaker zone of the microstructure and the foam damage progresses in layers perpendicular to the loading axis [13,16]. In the case of hydrostatic compression, one can also assume that the damage is initiated in a weaker beads and its progression depends on the stiffness of the neighbour beads and the stress distribution. It is clear that, following this hypothesis, the various propagation of the damage (depending on the foam sample microstructure) induces a variation of the axial strain comparatively to the radial strain and then a dispersion of the ratio  $K_r$ .

Several hypotheses were explored to explain the transverse isotropy of the deformation field. First, the dimensions of the sample – and more precisely the height to diameter ratio – can have an influence on the behaviour measured. It is well known that the height to diameter ratio can have an effect on the response of a specimen in the case of uniaxial compression. This effect may also be present in hydrostatic compression but several complementary hydrostatic compressions were done by using foam samples of different height to diameter ratios and their results show that this first hypothesis of scale effects have to be rejected. The second hypothesis is thus anisotropy of the foam which could be exacerbated under the loading of hydrostatic compression. The tests of uniaxial compressions have assumed the isotropy of the foam [16]; the gas under pressure (in hydrostatic compression) can however have a great influence on the response of the structure of the foam. Otherwise, a hypothesis has been already made that the viscoelastic behaviour of the foam is due to the coupling of effect of the pressurized gas and the structure of the cellular material. One also assumes that the manufactured microstructure is not exactly isotropic. The structure of the foam is carried out during the manufacturing of the foam blocks and the parameters of the industrial process vary as a function of the pre-set density. The block being moulded under pressure, the variable parameters of the moulding can induce a change of the microstructure and micro porosity of the foam which may be difficult to observe and estimate. This transverse isotropy can be sufficiently low to have no effect in the case of uniaxial compression but can be revealed in combining the effects of the multi-axial loading on the structure and of the gas under pressure.

## 5. Conclusion

A hydrostatic compression apparatus was designed to measure the foam response and obtain the variation of hydrostatic stress versus volumetric strain as functions of density and strain rate. High speed image techniques and associated analysis were implemented on this apparatus. The axial and radial strains of the foam sample were also determined; the strain tensor was then completely determined by using Image Processing and the stress tensor was easily obtained from the measurement of the pressure in the experiment chamber.

Hydrostatic compression tests have shown that polypropylene foam response includes a non-linear elastic behaviour followed by a stress plateau during which the material was progressively damaged. The final step is the foam densification. The non-linear

elastic stage and the plastic plateau were characterised and the compressibility modulus  $K$ , the yield stress  $\sigma_m$  and the tangent modulus  $E_T$  were identified. The sensitivity of the foam behaviour to the two parameters density and strain rate was underlined. More precisely, one could observe that the rise in density involves an increase in the compressibility modulus, the yield stress and the plastic plateau. The influence of the strain rate on the material response was also shown, with an increase in the compressibility modulus  $K$  and the yield stress  $\sigma_m$  with the rise in strain rate. These data will be useful to characterise mechanical model of macroscopic behaviour of polypropylene foam as a function of the strain rate and the foam density. In the first conclusion, this apparatus could become indispensable to complete the experimental database on cellular materials usually determined by the only test of uniaxial compression.

On the other hand, the analysis of these tests has shown a non-linear elastic behaviour of this foam under hydrostatic loading and the transverse isotropy of the response of this polypropylene foam whereas previous studies [16] displayed its classical behaviour, which is an isotropic behaviour with an initial linear-elastic response, under uniaxial compression. The main hypothesis developed to explain the non-linear elastic behaviour is the coupling between the bead and cell structure response and the gas enclosed inside the sample and flowing through the microstructure walls. Furthermore, the foam microstructure is defined during the industrial process and may be slightly anisotropic. During the plastic plateau, the progression of the damage depends on this foam microstructure and the distribution of the stress in the sample. The transversely isotropic response can be only highlighted under hydrostatic compression because the pressure conditions in the microstructure are strongly different from the one assumed in the case of uniaxial loading.

Finally, the hydrostatic compression apparatus, initially designed to complete data on the macroscopic behaviour of cellular materials, has revealed a change of behaviour of the polypropylene foam under hydrostatic loading because this apparatus was instrumented with complementary measurement tools (high speed camera and image processing method). To check these new results and the associated hypotheses on the micromechanisms, it seems necessary to continue in this investigation by using techniques that can reveal physical phenomena at the microstructural scale. The use of microtomographic technique and thermal analysis during hydrostatic compression could provide complementary observations which can demonstrate the suspected deformation mechanisms.

## Acknowledgements

I would like to thank N.J. Mills for helping to improve the final version of the paper.

## References

- [1] Gibson L, Ashby F. Cellular solids. Structures and properties. Edition: Cambridge Solid State Science Series. Cambridge University Press; 1997.
- [2] Mills NJ, Fitzgerald C, Gilchrist A, Verdejo R. Polymer foams for personal protection: cushions, shoes and helmets. *Composites Science and Technology* 2003;63(16):2389–400.
- [3] Viot P. Polymer foams to optimize passive safety structures in Helmets. *International Journal of Crashworthiness* 2007;12(03):299–310.
- [4] Gibson LJ, Zhang J, Shercliff TL. Failure surface for cellular materials under multiaxial loads I. Modeling. *International Journal of Mechanical Science* 1989;31(9):635–63.
- [5] Zhang J, Kikuchi N, Li V, Yee A, Nuscholtz G. « Constitutive modeling of polymeric foam material subjected to dynamic crash loading ». *International Journal of Impact Engineering* 1998;21(5):369–86.
- [6] Triantafyllou TC, Zhang J, Shercliff TL, Gibson LJ, Ashby MF. Failure surfaces for cellular materials under multiaxial loads—II. Comparisons of models with experiment. *International Journal of Mechanical Sciences* 1989;31(9):665–78.
- [7] Miller RE. A continuum plasticity model of the constitutive and indentation behaviour of foamed metals. *International Journal of Mechanical Sciences* 2000;42(4):729–54.
- [8] Deshpande VS, Fleck NA. Isotropic constitutive models for metallic foams. *Journal of the Mechanics and Physics of Solids* 2000;48:1253–83.
- [9] Tagarielli VL, Deshpande VS, Fleck NA, Chen C. A constitutive model for transversely isotropic foams, and its application to the indentation of balsa wood. *International Journal of Mechanical Sciences* 2005;47(4–5):666–86.
- [10] Chen C, Deshpande VS, Fleck NA. A constitutive model for a transversely isotropic compressible solid: user manual for a UMAT in ABAQUS. Cambridge University Engineering Department internal report. CUED/C-MICROMECH/TR.93; 2003.
- [11] Hallquist JO. LS-DYNA3D Theoretical manual. LSTC Report 1018; 1994.
- [12] Jin H, Lu Wei-Yang, Scheffel S, Hinnerichs T, Neilsen M. Full-field characterization of mechanical behaviour of polyurethane foams. *International Journal of Solids and Structures* 15 October 2007;44(21):6930–44.
- [13] Viot P, Beani F, Lataillade J-L. Polymeric foam behaviour under dynamic compressive loading. *Journal of Material Science* 2005;40:5829–37.
- [14] Bouix R, Viot P, Lataillade JL. Phenomenological study of cellular material behavior under dynamic loadings. In *eurodynat 2006*. *Journal de Physique IV* 2006;134(2006):109–16.
- [15] Froustey C, Lambert M, Charles JL, Lataillade JL. Design of an impact loading machine based on a flywheel device: application to the fatigue resistance of the high rate pre-straining sensitivity of aluminium alloys. *Experimental Mechanics* 2007;. doi:10.1007/s11340-007-9082-4.
- [16] Bouix R, Viot P, Lataillade JL. Polypropylene foam behaviour under dynamic loadings: Strain rate, density and microstructure effects. *International Journal of Impact Engineering* 2009;36(2):329–42.
- [17] Viot P, Bernard D, Plougonven E. Polymeric foam deformation under dynamic loading by the use of the microtomographic technique. *Journal of Materials Science* 2007;. doi:10.1007/s10853-006-1422-8.
- [18] Masso Y, Moreu, Mills NJ. Rapid hydrostatic compression of low-density polymeric foams. *Polymer Testing* 2004;23:312–22.